Neuro-Oncology

XX(XX), 1–11, 2021 | doi:10.1093/neuonc/noab034 | Advance Access date 13 February 2021

Ultra high-risk PFA ependymoma is characterized by loss of chromosome 6q

Lorena V. Baroni,[†] Lakshmikirupa Sundaresan,[†] Ayala Heled, Hallie Coltin, Kristian W. Pajtler, Tong Lin, Thomas E. Merchant, Roger McLendon, Claudia Faria, Molly Buntine, Christine L. White, Stefan M. Pfister, Mark R. Gilbert, Terri S. Armstrong, Eric Bouffet, Sachin Kumar, Michael D. Taylor, Kenneth D. Aldape, David W. Ellison, Nicholas G. Gottardo, Marcel Kool, Andrey Korshunov, Jordan R. Hansford,[‡] and Vijay Ramaswamy[‡]

Division of Haematology/Oncology, Hospital for Sick Children, Toronto, Ontario, Canada (L.B., H.C., E.B., V.R.); Programme in Developmental and Stem Cell Biology, Arthur and Sonia Labatt Brain Tumour Research Centre, Hospital for Sick Children, Toronto, Ontario, Canada (L.B., L.S., H.C., A.H., S.K., M.D.T., V.R.); Hopp Children's Cancer Center Heidelberg (KiTZ), Heidelberg, Germany (K.W.P., S.M.P., M.K., A.K.); Division of Pediatric Neuro-Oncology, German Cancer Research Center (DKFZ), German Cancer Consortium (DKTK), Heidelberg, Germany (K.W.P., S.M.P., A.K., M.K.); Department of Pediatric Oncology and Hematology, University Hospital Heidelberg, Heidelberg, Germany (K.W.P., S.M.P.); Department of Biostatistics, St. Jude Children's Research Hospital, Memphis, Tennessee, USA (T.L.); Department of Radiation Oncology, St. Jude Children's Research Hospital, Memphis, Tennessee, USA (T.E.M.); The Preston Robert Tisch Brain Tumor Center, Duke University, Durham, North Carolina, USA (R.M.); Division of Neurosurgery, Centro Hospitalar Lisboa Norte, Hospital de Santa Maria, Lisbon, Portugal (C.F.); Hudson Institute of Medical Research, Clayton, Australia (M.B., C.L.W.); Neuro-Oncology Branch, National Cancer Institute, Bethesda, Maryland, USA (M.R.G., T.S.A.); Division of Neurosurgery, Hospital for Sick Children, Toronto, Ontario, Canada (M.D.T.); Center for Cancer Research, National Cancer Institute, Bethesda, Maryland, USA (K.D.A.); Department of Pathology, St. Jude Children's Research Hospital, Memphis, Tennessee, USA (D.W.E.); Department of Paediatric Oncology and Haematology, Perth Children's Hospital, Perth, Australia (N.G.G.); Princess Maxima Center for Pediatric Oncology, Utrecht, the Netherlands (M.K.); Clinical Cooperation Unit Neuropathology, German Cancer Research Center (DKFZ), Heidelberg, Germany (A.K.); Children's Cancer Centre, Royal Children's Hospital; Murdoch Children's Research Institute; Department of Pediatrics, University of Melbourne; Monash University, Melbourne, Australia (J.R.H.); Department of Medical Biophysics, University of Toronto, Toronto, Ontario, Canada (V.R.)

[†] These authors contributed equally to this work.

[‡] Denotes co-senior authors.

Corresponding Authors: Vijay Ramaswamy, MD, PhD, Division of Haematology/Oncology, Hospital for Sick Children, 555 University Ave, Toronto M5G 1X8, ON, Canada (vijay.ramaswamy@sickkids.ca); Jordan R. Hansford, MBBS FRACP, Children's Cancer Centre, Royal Children's Hospital Melbourne, Parkville, Victoria 3052, Australia (Jordan.Hansford@rch.org.au).

Abstract

Background. Within PF-EPN-A, 1q gain is a marker of poor prognosis, however, it is unclear if within PF-EPN-A additional cytogenetic events exist which can refine risk stratification.

Methods. Five independent non-overlapping cohorts of PF-EPN-A were analyzed applying genome-wide methylation arrays for chromosomal and clinical variables predictive of survival.

Results. Across all cohorts, 663 PF-EPN-A were identified. The most common broad copy number event was 1q gain (18.9%), followed by 6q loss (8.6%), 9p gain (6.5%), and 22q loss (6.8%). Within 1q gain tumors, there was significant enrichment for 6q loss (17.7%), 10q loss (16.9%), and 16q loss (15.3%). The 5-year progression-free survival (PFS) was strikingly worse in those patients with 6q loss, with a 5-year PFS of 50% (95% CI 45%-55%) for balanced tumors, compared with 32% (95% CI 24%-44%) for 1q gain only, 7.3% (95% CI 2.0%-27%) for 6q loss only and 0 for both 1q gain and 6q loss ($P = 1.65 \times 10^{-13}$). After accounting for treatment, 6q loss remained the most significant independent predictor of survival in PF-EPN-A but is not in PF-EPN-B. Distant relapses were more common in 1q

gain irrespective of 6q loss. RNA sequencing comparing 6q loss to 6q balanced PF-EPN-A suggests that 6q loss forms a biologically distinct group.

Conclusions. We have identified an ultra high-risk PF-EPN-A ependymoma subgroup, which can be reliably ascertained using cytogenetic markers in routine clinical use. A change in treatment paradigm is urgently needed for this particular subset of PF-EPN-A where novel therapies should be prioritized for upfront therapy.

Key Points

1. 1q gain PF-EPN-A have a distinct cytogenetic profile enriched for 6q loss, 10q loss, and 16q loss.
2. Loss of 6q defines a group of PF-EPN-A with a dismal survival independent of either treatment or 1q gain.
3. Distant relapses are more common in 1q gain tumors.

Importance of the Study

We identify an ultra high-risk subset of posterior fossa ependymoma subgroup characterized by 6q loss, comprising 9% of all PFA ependymoma. Loss of 6q predicts a very poor survival independent of 1q status and is a highly significant predictor of progression-free survival and overall survival after accounting for treatment variables. This group should be prioritized for upfront experimental approaches due to their rapid progression and very poor survival.

Posterior fossa ependymoma (PF-EPN) are comprised of three distinct molecular groups termed PF-EPN-A, PF-EPN-B, and PF-EPN-SE with distinct demographics, cytogenetics, epigenetics, and outcomes.[1–3] PF-EPN-B characterized by frequent chromosomal arm-level gains and losses are the predominant subgroup observed in adults and have an overall excellent prognosis.[4–7] PF-EPN-A have a relatively silent genome, with a paucity of recurrent somatic nucleotide variants and only 1q gain as a commonly observed chromosomal arm-level copy number aberration.[8,9] PF-EPN-A are found predominantly in young children and are associated with poor prognosis.[8,10] Within each of these groups, there is substantial heterogeneity, with 9 subgroups identified within PF-EPN-A and 5 subgroups identified within PF-EPN-B.[4,9] Current risk stratification for PF-EPN is based on the extent of resection and administration of upfront radiation, where incompletely resected and/or non-irradiated PF-EPN-A have a dismal outcome.[10–12] As such, children as young as 1 year of age are treated with aggressive surgical resection and postsurgical adjuvant radiotherapy, which are associated with long-term neurocognitive impairment.[12]

Although survival of completely resected PF-EPN-A who received postoperative radiotherapy have a progression-free survival (PFS) of around 60%-70%, gain of 1q has been shown across multiple studies to be a highly prognostic independent marker of a poor outcome within PF-EPN-A, including the recently reported Children's Oncology Group (COG) study ACNS0121.[11,13–16] Interestingly within PF-EPN-B, 1q gain has no prognostic value, suggesting a clear group specificity, but also suggests that previously identified markers across all ependymoma require re-examination in a group-specific manner.[4] Indeed, some markers such as 6q loss have been identified as frequent events in ependymoma and in some studies a marker of excellent prognosis, however, these studies have not been re-analyzed in a group-specific manner.[16–24]

There is additional heterogeneity within PF-EPN-A, where 9 subgroups have been identified, with one subgroup, PFA1c being enriched for 1q gain and harboring a poor prognosis, and PFA-2c which as an excellent outcome.[9] To extend these findings, we evaluated if cytogenetic markers may provide important prognostic value that complements these previous studies, specifically we sought to investigate if cytogenetic markers of prognosis with PF-EPN-A ependymoma, specifically 1q gain PF-EPN-A could provide additional risk stratification.

Methods

Patient Cohort

Six hundred and sixty-three PFA (PF-EPN-A) were identified through the Global Ependymoma Network of Excellence (GENE), the Australian & New Zealand Children's Haematology/Oncology Group, St. Jude's Children's Research Hospital, Burdenko Neurosurgical Institute, and the CERN Foundation, all previously profiled using genome-wide DNA methylation profiling and where copy number plots could be interpreted (GSE104210).[9,10] Both frozen and formalin-fixed paraffin embedded (FFPE) samples were collected from diagnosis. Of these 663 subjects, full survival information was available in 602. A subtotal resection was defined as more than 5 mm postoperative residual on the postoperative MRI. A previously reported

cohort of 212 PFB (PF-EPN-B) tumors was included for a re-analysis of copy number aberrations.[4] Samples were all collected in accordance with the approval of the Hospital for Sick Children Research Ethics Board and local institutional research ethics boards.

Genome-Wide DNA Methylation Profiling

Samples were analyzed on the Illumina Infinium HumanMethylation450 or HumanMethylationEPIC array at the PM-OICR Translational Genomics Laboratory and Princess Margaret Genomics Centre (Toronto, Ontario), the German Cancer Research Center (Heidelberg, Germany), or the Hudson Research Institute (Melbourne, Australia) according to the manufacturer's instructions and pre-processed as previously described.[8] PF-EPN-A status was determined using the Heidelberg brain tumor classifier (https://www.molecularneuropathology.org/mnp) as previously described.[8,25] Distance between samples was calculated using Pearson correlation coefficient as the distance measure and the same distance matrix was used to perform the t-distributed stochastic neighbor embedding (tSNE) analysis using the Rtsne package version 0.11.17. The following non-default parameters were used: theta = 0, is_distance = T, pca = F, max_iter = 10 000, perplexity = 30. All analyses were conducted in the R Statistical Environment (v4.0.2).

Copy Number Inference From Methylation Arrays and Identification of Recurrent Broad Events

Copy number segmentation was performed from genome-wide methylation arrays using the conumee package (v0.99.4) in the R statistical environment (v4.0.2) as previously described.[26,27] Broad copy number events were determined using visual inspection of copy number plots and significance of the frequency of each broad event was tested using the exact binomial test, and applying the GISTIC broad event analysis.[28]

Transcriptome Sequencing Analysis

RNA sequencing was performed using ribodeplete library preparation to a read depth of 50 million reads per sample on the NextSeq platform at the Centre for Applied Genomics at the Hospital for Sick Children. The quality of the sequence reads was assessed by FASTQC v0.72 and Trim Galore v0.6.3 (http://www.bioinformatics.babraham.ac.uk/projects). The reads were mapped against human reference genome hg38 reads using HISAT2 algorithm v2.1.0 and featureCounts v1.6.3 was employed to obtain the counts from the uniquely aligned reads.[29,30] Further, differential expression analysis between the subgroups was performed using R/Bioconductor package DESeq2 v1.26.0 and log-transformed for exploratory analysis, where an adjusted *P* value <.05 was considered to be statistically significant. Principal component analysis (PCA) plot was using pcaMethods R package, the genes were scaled based on unit variance method and principal components were calculated with imputation and singular value decomposition (SVD) iteratively. Confidence ellipses were calculated using FactoMineR R package (v2.3). Heatmaps were constructed using ComplexHeatmap R package (v2.5.1). The differentially expressed chromosomal regions were determined using PREDA R package. Regions with FDR (false discovery rate) < 0.05 were considered to be differentially regulated. The genes were ranked using the $\log_{10}$ *P* values multiplied by sign of fold change from DESeq2 analysis. Enrichment analysis was carried out using pre-ranked gene set enrichment analysis (GSEA) and was run with the C1 (positional), C2 (canonical pathways), and C5 (gene ontology).[31] Hallmark gene sets were visualized using EnrichmentMap in Cytoscape.[31] The hypoxia scores were computed based on previously reported mRNA-based hypoxia signatures along with the Hallmark_hypoxia signature from GSEA. The logCPM expression data derived using edgeR for all the genes in the hypoxia signatures were extracted for 6q balanced and 6q loss samples. To compare hypoxia among the subgroups, each patient was evaluated against the median gene abundance for the same gene in all the samples. When the abundance was greater than the median, it was assigned a score of 1 whereas abundance lower than the median was assigned a score of –1. The hypoxia score for each patient was computed as the sum of scores for each gene in a given hypoxia signature. RNA sequencing data have been deposited into GEO with accession number GSE164292.

Statistical Analysis

PFS and overall survival were analyzed by the Kaplan-Meier method and *P* values reported using the log-rank test. Associations between covariates and risk groups were tested by the Fisher's exact test. Univariable and multivariable cox proportional hazard regression was used to estimate hazard ratios including 95% confidence intervals (CI). The proportional-hazards assumption was tested using the cox.zph function in the survival package and graphical inspection of Schoenfeld residual plots and was not statistically significant for any of the covariates. A multivariable logistic regression model estimated the associations between the candidate predictor variables (1q status, 6q status, extent of resection, radiotherapy, age at diagnosis) and the odds of distant metastatic relapse, with appropriate model fitting using the post-estimation Hosmer-Lemeshow goodness-of-fit test. All statistical analyses were performed using the R statistical environment (v4.0.2), R packages survival (v3.2-7), and ggplot2 (v3.3.2).

Results

Demographics and Cytogenetic Landscape of PF-EPN-A

In total, 663 PF-EPN-A samples with available DNA copy number data were identified, where 124 harbored 1q gain (18.7%) and 538 had a balanced 1q status (81.3%). Demographics of the cohort are summarized in Table 1.

Full survival data were available in 602 subjects with PF-EPN-A. Demographics and treatment details of the overall cohort comparing 1q gain and 1q balanced are listed in Table 1. The median age across the entire cohort was 3 (IQR 1.68-5), with the median age of 1q gain patients being significantly older compared to a balanced 1q state (1q gain median age 5.99, IQR 3.34-8.02; 1q balanced median age 2.42, IQR 1.4-4; $P = 2.2 \times 10^{-16}$). Gender ratio was not significantly different where 20.1% of males and 17.3% of females harbored 1q gain ($P = .4$). Rates of incomplete resection were nearly identical between 1q gain and 1q balanced (1q gain –36%, 1q balanced 37.4%,

Table 1 Demographics and Cytogenetic Features of 1q Gain and 6q Loss PF-EPN-A

	Total Cohort (n = 662)	Balanced (n = 503)	1q Gain Only (n = 102)	6q Loss Only (n = 35)	1q Gain and 6q Loss (n = 22)	*P* Value[d]
Age (median + IQR)[a,e]	4.1 (1.69-5)	2.25 (1.33-4)	5.0 (3-8)	5 (3.1-7.5)	6 (3.4-8.0)	4.4×10^{-8}
Age group[b]						
<3 years (n = 379)	47.6%	92.9%	5.2%	1.3%	0.6%	2.2×10^{-16}
3-10 (n = 187)	46.3%	64%	22.8%	8.3%	5.0%	
10-17 (n = 30)	4.9%	37.5%	43.8%	9.4%	9.4%	
>17 (n = 6)	1.2%	37.5%	25%	25%	12.5%	
Male gender[f]	58.4%	57.7%	64.4%	61.8%	45.5%	.35
Upfront XRT[g]	79.2%	76.6%	91.6%	83.3%	73.7%	.0097
Chemotherapy[g]	51.4%	52.8%	48.9%	38.7%	52.6%	.46
Incomplete resection[g]	37.1%	37.3%	33.7%	38.7%	47.4%	.71
Pattern of relapse[h]						
Local tumor bed	64.7%	67.2%	54.8%	83.3%	38.5%	.040
Metastatic (combined ± distant only)	35.3%	32.8%	45.2%	16.7%	61.5%	
Total chromosomal alterations[c] (mean + SD)	1.06 ± 2.40	0.74 ± 2.08	1.77 ± 2.77	3.02 ± 3.28	1.95 ± 3.29	2.5×10^{-5}
0	69.8%	81.5%	33.3%	17.1%	54.5%	
1	8.0%	0.8%	38.2%	25.7%	4.5%	
2	9.5%	8.9%	7.8%	17.1%	18.2%	
>3	12.7%	8.7%	20.6%	40%	22.7%	
Broad cytogenetic alterations (>2.5% total)						
Whole Chr 2 gain	2.4%	2.6%	2.9%	0%	0	.87
Whole Chr 7 gain	3.0%	1.6%	7.8%	5.7%	9.1%	.0008
Whole Chr 8 gain	4.1%	3.6%	5.9%	2.9%	9.1%	.28
9p gain	6.5%	5.4%	12.7%	5.7%	4.5%	.06
9q gain	5.9%	5.2%	10.8%	2.9%	4.5%	.19
10q loss	5.4%	1.2%	17.6%	25.7%	13.6%	3.7×10^{-14}
Whole Chr 11 gain	3.6%	3.4%	6.9%	0	0	.2
16q loss	3.5%	0.2%	15.7%	8.6%	13.6%	3.2×10^{-13}
17p loss	2.3%	0.8%	1.0%	25.7%	4.5%	1.3×10^{-8}
17q gain	2.7%	2.6%	3.9%	2.9%	0	.81
Whole Chr 19 gain	3.8%	4.0%	3.9%	2.9%	0	1
Whole Chr 19 loss	3.2%	2.4%	5.9%	5.7%	4.5%	.11
22q loss	6.8%	5.8%	5.9%	25.7%	4.5%	.0019

Abbreviations: IQR, interquartile range; SD, standard deviation; XRT, external beam irradiation.
[a]1q gain vs 6q loss—$P = .15$, 1q gain vs 1q gain/6q loss—$P = .82$, 6q loss vs 1q gain/6q loss—$P = .87$ (Tukey contrasts).
[b]Percentages by row (% within each age group).
[c]Excludes 1q and 6q.
[d]*P* values across balanced, 1q gain, 6q loss, and 1q gain/6q loss columns.
[e]Age available in 654 cases.
[f]Gender available in 660 cases.
[g]Radiotherapy, chemotherapy, extent of surgical resection, and survival available in 602 cases.
[h]Pattern of relapse available in 187 progression events.

P = .83). Upfront radiotherapy was significantly more common in patients harboring a tumor with 1q gain, where 77.1% of 1q balanced patients received upfront radiotherapy compared to 88.6% for 1q gain (P = .0066) (Table 1). As previously reported, survival was significantly worse in 1q gain patients, with 5-year PFS for 1q balanced was 46.7% (95% CI 42%-51.9%) compared to 26.1% (95% CI 19%-35.8%) for 1q gain patients ($P = 7.9 \times 10^{-6}$); and 10-year PFS for 1q balanced was 41.4% (95% CI 36.4%-46.4%) compared to 16.5% (95% CI 10.2%-26.7%) for 1q gain patients ($P = 4.2 \times 10^{-6}$). When restricting the analysis to only patients who achieved a complete resection and received upfront radiotherapy, the difference in survival is even more striking with 5-year PFS for 1q balanced of 63.9% (95% CI 57.6%-70.9%) and 1q gain of 24.8% (15.8%-39.1%) ($P = 1.36 \times 10^{-11}$). Within the 1q gain group, a multivariable cox regression analysis revealed that when correcting for age, extent of resection, gender, and upfront radiotherapy, only male gender remained a significant predictor of poor outcome (Supplementary Table 1).

Cytogenetic Landscape of 1q Gain PF-EPN-A

In order to identify the cytogenetic events within PF-EPN-A, broad copy number changes were inferred from the genome-wide methylation analysis (Figure 1C, D, Table 1). No significant focal events were identified across all PF-EPN-A, consistent with previous studies. Across all PF-EPN-A, 1q gain was the most frequent broad copy number event observed (18.9%), with 6q loss (8.6%), 9p gain (6.5%), 9q gain (5.9%), 10q loss (5.4%), and 22q loss (6.8%) being the only other significant events occurring at a frequency higher than 5% (Table 1). However, when stratifying the analysis by 1q status, we observed 6q loss being significantly enriched with a frequency of 17.7%, compared to 6.6% within the 1q balanced group (Figure 2A,

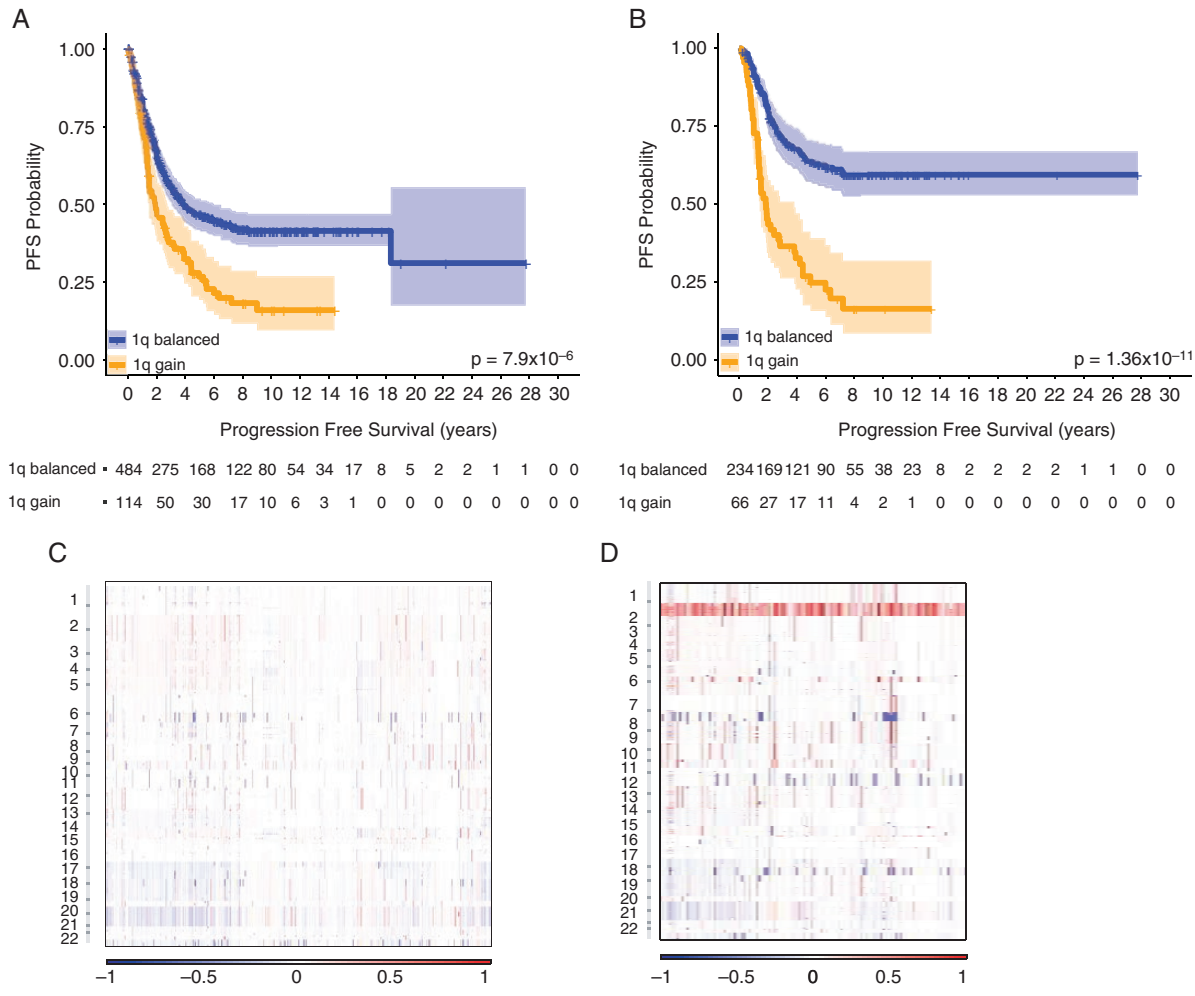

Fig. 1 Clinical and cytogenetic landscape of 1q gain PF-EPN-A. Kaplan-Meier progression-free survival analysis of 1q status across (A) all PF-EPN-A and (B) only completely resected and radiated PF-EPN-A. Copy number heatmaps comparing (C) 1q balanced PF-EPN-A and (D) 1q gain PF-EPN-A where blue indicates loss, and red indicates gain. P values determined using the log-rank test, and shaded areas around each curve represent 95% confidence intervals.

$P = 2.5 \times 10^{-4}$). Other events significantly enriched in more than 10% of 1q gain PF-EPN-A include 16q loss (1q gain 15.3% vs 1q balanced 0.74%; $P = 4.1 \times 10^{-12}$), 10q loss (1q gain 16.9% vs 1q balanced 2.8%; $P = 5.4 \times 10^{-8}$) and 9p gain (1q gain 11.3% vs 1q balanced 5.4; $P = .049$). The median number of arm-level copy number events was significantly higher in both 1q gain and 6q loss compared to a balanced genome, (1q/6q harbor 0.74 arm-level copy number events per tumor, 6q loss only: 3.02, 1q gain only: 1.77, 1q gain/6q loss: 1.95, $P = 2.5 \times 10^{-5}$, Table 1), with no significant difference between 1q gain and 6q loss ($P = .08$). Analysis of a previously reported PF-EPN-B cohort revealed 6q loss in 65% of samples with no association with 1q gain ($P = .56$).[4] FISH (fluorescence in situ hybridization) was performed where the material was available demonstrating 6q loss, confirming that both 1q gain and 6q loss can be identified by FISH in addition to genome-wide methylation profiling (Figure 2B). tSNE analysis does not show distinct clustering of 6q loss PF-EPN-A, with representation across both PFA1 and PFA2 as previously described (Supplementary Figure S1).[9] Median age at diagnosis was significantly higher overall in patients with 6q loss compared to 6q balanced but was not significantly different from 1q gain (Figure 2C, 6q loss: 5-year IQR 3-7.5; 6q balanced: 2.8-year IQR 1.5-4.85, $P = 2.5 \times 10^{-7}$).

Prognostic Cytogenetic Markers Within 1q Gain PF-EPN-A

In order to determine if the three other recurrent cytogenetic events within 1q gain PF-EPN-A harbor prognostic significance, a univariable survival analysis was performed stratifying by 6q loss, 16q loss, or 10q loss. Neither PFS nor overall survival was significantly different when stratifying by copy number state of 10q or 16q. However, 6q loss was highly prognostic within 1q gain PF-EPN-A, with a 5-year PFS of 0 compared to 32.4% (95% CI 23.7%-44.2%) for 6q balanced (Figure 2D, $P = 6 \times 10^{-5}$). Across all PF-EPN-A, and restricted to 1q balanced PFA, 6q loss remained highly prognostic as well, suggesting this may be an independent marker of poor outcome across all PF-EPN-A including those restricted to having achieved a complete resection followed by upfront radiotherapy (Figure 2E, Supplementary Figure S2). Loss of 6q portended to a more rapid progression, with a median PFS of 1.42 years compared to 3.92 years for 6q balanced. When restricted to only 1q gain patients, 6q loss had a median PFS of 0.75 years compared to 2.42 years for 6q balanced.

In order to determine the prognostic relevance of 6q loss across all PF-EPN-A, we performed a multivariable cox regression analysis including age, incomplete surgical resection, upfront radiotherapy, male gender, 1q gain, and 6q loss. When correcting for all factors, the most powerful predictor of poor PFS across all PF-EPN-A is 6q loss (Table 2, HR 2.78, 95% CI 2.00-3.86, $P = 9.8 \times 10^{-10}$). Consistent with previous studies, an incomplete resection, absence of upfront radiotherapy, male gender, and 1q gain were all independently significant prognostic markers for poor PFS and overall survival (Table 2). Within the 1q gain group, 6q remained a very powerful predictor of the outcome when accounting for the extent of resection, upfront radiotherapy, and male gender (Supplementary Table 2, HR 3.26, 95% CI 1.88-5.66, $P = 2.5 \times 10^{-5}$). Two patients with 6q loss without progression after 2 years were identified, a 4-year-old male with a PFS of 2.91 years with a calibrated score of 0.98 for a PF-EPN-A, and a 51-year-old female with a PFS of 9.5 years, with a low confidence PF-EPN-A (calibrated score 0.64) which may potentially represent an outlier. Only five patients over age 18 were identified across the entire cohort precluding an analysis of cytogenetic and prognostic markers restricted to adult PF-EPN-A. In a re-analysis of a previously reported PF-EPN-B cohort,[4] 6q loss was not a significant predictor of either PFS or overall survival in either a univariable (HR 1.55, 95% CI 0.73-3.32, $P = .26$) or multivariable analysis when correcting for the extent of resection, upfront radiotherapy, male gender and age (HR 1.28, 95% CI 0.59-2.79, $P = .53$) (Supplementary Table 3).

The pattern of relapse was available in 187 progression events. The first site of relapse was the surgical cavity in 121, metastatic only in 52, and combined surgical cavity plus metastasis in 14. When stratifying by copy number aberration, distant relapses were more common in tumors harboring 1q gain than those without (1q balanced: 69.2% local, 23.1% distant only, 7.7% combined vs 1q gain: 50% local, 43.2% distant only, 6.8% combined, $P = .033$, Figure 2F). Overall, tumors harboring 6q loss relapsed most frequently in the surgical cavity (6q balanced: 64.7% local, 26.9% distant only, 8.3% combined, 6q loss: 64.5% local, 32.3% distant only, 3.2% combined, $P = .56$). Interestingly, when restricting the analysis to only 6q loss, those with 6q loss only most frequently recurred locally (83.3% local, 16.7% distant only) and those harboring both 1q gain and 6q loss recurred with distant failure (38.5% local, 53.8% distant only, 7.7% combined, $P = .03$, Figure 2F, Table 1). A multivariable regression model confirmed that 1q gain was a significant predictor of distant relapse even when accounting for extent of surgical resection, upfront radiotherapy, age at diagnosis, and 6q loss (Table 3).

6q Loss PF-EPN-A Is a Biologically Distinct Group

In order to identify potential targets on chromosome 6q which may be driving the more aggressive behavior in this subset, RNA sequencing was performed across 5 samples with balanced 6q status, and 5 samples harboring 6q loss with balanced 1q status. Unsupervised hierarchical clustering, PCA, and tSNE analysis of the top differentially expressed genes show clear segregation of 6q loss from 6q balanced samples (Figure 3A, Supplementary Figures S3 and S4). When we repeated this analysis excluding genes on 6q, a similar pattern of segregation is observed (Supplementary Figure S3). Differentially expressed genes plotted as a function of chromosomal position reveals downregulation of genes across the entire arm of 6q being significant, however, an analysis of the top 25 downregulated genes restricted to 6q did not identify a clear tumor suppressor or a set of genes downregulated on 6q which would account for the aggressive behavior (Figure 3B, Supplementary Figures S5 and S6). GSEA comparing 6q loss to 6q balanced gene expression revealed

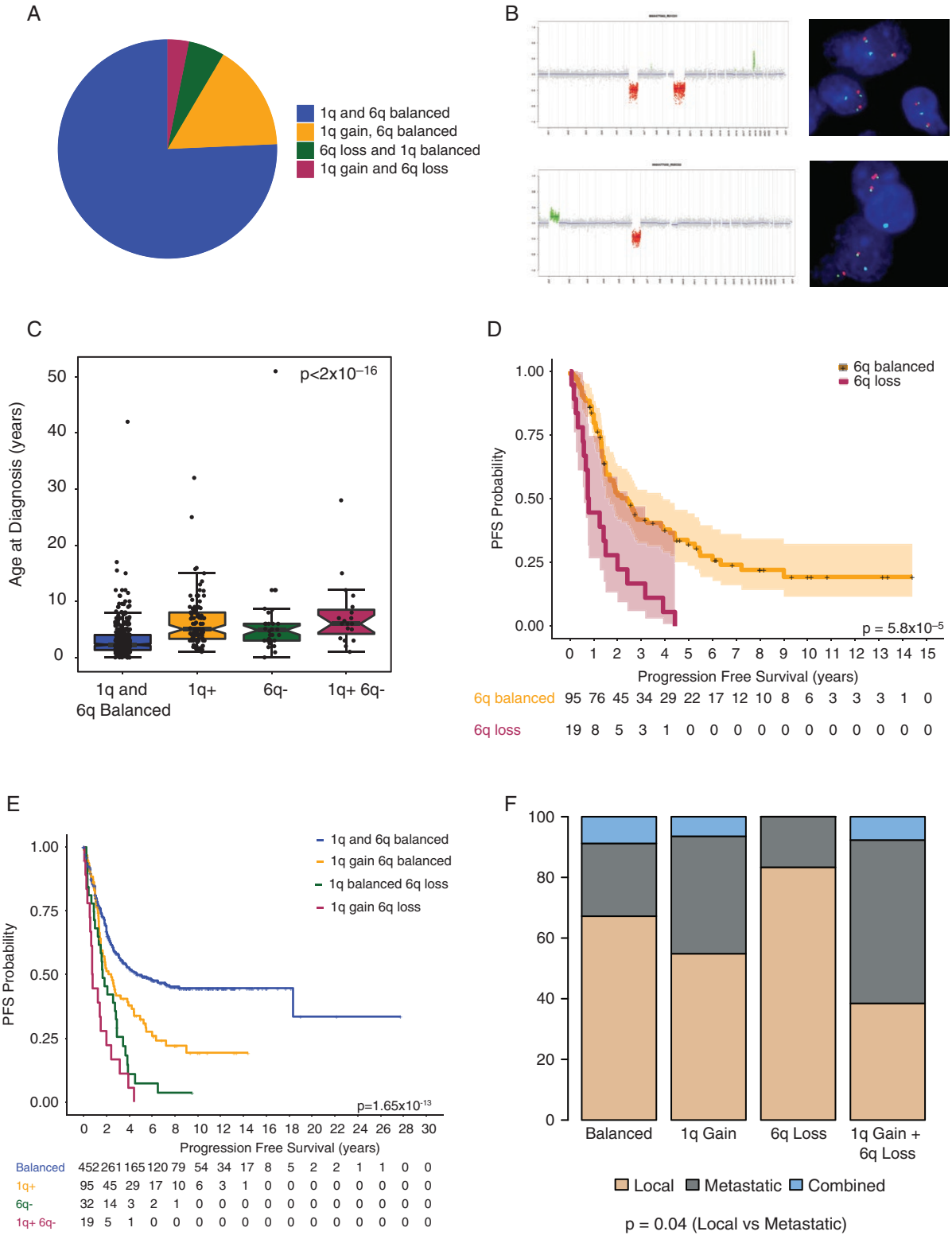

Fig. 2 Clinical features of 6q loss ependymoma. (A) Percentage distribution of 1q and 6q status across all PF-EPN-A. (B) Representative copy number profile and corresponding FISH of two tumors showing correlation between the two methods. Aqua—probe to 6q; Red 17p and Green 17q. (C) Age distribution stratified by 1q and 6q status across all PF-EPN-A. Post-hoc comparison using Tukey contrast for age—All bal vs 1q+: $P < 1 \times 10^{-5}$, All bal vs 6q−: $P = 1.5 \times 10^{-5}$, All bal vs 1q+6q−: $P < 1 \times 10^{-5}$, 1q+ vs 6q−: $P = 1$, 1q+ vs 1q+6q−: $P = .76$, 6q− vs 1q+6q−: $P = .68$. Kaplan-Meier survival analysis stratified by 1q and 6q status across (D) 1q gain PF-EPN-A only, (E) all PF-EPN-A. *P* values determined using the log-rank test. (F) Pattern of relapse stratified by 1q and 6q status with the *P* value determined comparing local relapse to any distant relapse.

Table 2 Multivariable Analysis of Survival in PF-EPN-A

Variable	HR	95% CI	*P* Value
Progression-free survival (n = 576)			
Age	0.98	0.94-1.01	.13
Incomplete resection	1.74	1.38-2.19	**2.42×10^{-6}**
Upfront radiotherapy	0.50	0.38-0.65	**4.2×10^{-7}**
Male gender	1.40	1.10-1.77	**.0055**
1q gain	1.84	1.39-2.42	**1.48×10^{-5}**
6q loss	2.78	2.00-3.86	**9.8×10^{-10}**
Overall survival (n = 574)			
Age	0.98	0.93-1.02	.27
Incomplete resection	1.56	1.16-2.11	**.0037**
Upfront radiotherapy	0.62	0.44-0.87	**.0060**
Male gender	1.33	0.98-1.80	.063
1q gain	1.90	1.34-2.70	**.00033**
6q loss	2.39	1.60-3.58	**2.4×10^{-5}**

Bold values indicates $P < .05$.

Table 3 Multivariable Analysis of Predictors of Distant Relapse in PF-EPN-A

	Adjusted Odds Ratio	95% CI	*P* value
Age (continuous)	1.03	0.93-1.14	.543
Male gender	0.75	0.39-1.44	.388
Incomplete resection	0.67	0.34-1.30	.231
Upfront radiotherapy	1.07	0.51-2.21	.861
1q gain	2.42	1.05-5.60	**.039**
6q loss	1.09	0.71-1.68	.693

Post-estimation Hosmer-Lemeshow goodness-of-fit test ($P = .9526$) demonstrating appropriate model fitting.
Complete data available in 181 progression events.
Bold values indicates $P < .05$.

various upregulated pathways in 6q loss including several pathways pertaining to immune response, hypoxia, FGFR (fibroblast growth factor receptor) signaling, TGFβ (transforming growth factor beta) signaling, and angiogenesis with motility-related pathways significantly downregulated (Figure 3C). Previously, it has been shown that PF-EPN-A are highly dependent on a hypoxic microenvironment which in turn controls metabolic intermediates.[32] Consistent with this, we observe that 6q loss tumors are highly enriched for six previously described hypoxia signatures compared to 6q balanced tumors, however, differential expression of HIF1α was not observed (Supplementary Figures S5 and S7).[33–39]

Discussion

Herein we show that across all PF-EPN-A, an ultra high-risk group comprises 10% of all patients and is defined by loss of chromosome 6q, independent of treatment or 1q status. Although present in a subset of PF-EPN-A, the rapid progression and near-ubiquitous relapses within this group suggest that this group warrants a new upfront treatment approach.

Our results are highly concordant with a previous analysis of PF-EPN-A where 9 groups of PF-EPN-A were identified.[9] Within these 9 groups, PFA1c is highly enriched for 1q gain and harbors a poor prognosis independent of 1q status. Loss of 6q is also significantly enriched in PFA1c but is present across all PF-EPN-A and was suggested in this previous study to be a univariate predictor of poor outcome. Our results extend on these findings, whereby a more granular analysis of known risk factors reveals that 6q loss represents a highly aggressive subset of PF-EPN-A, irrespective of treatment or 1q gain. More importantly, this aberration represents a simple, and universally applicable marker to identify the highest risk group of PF-EPN-A. Genome-wide DNA methylation supports 6q

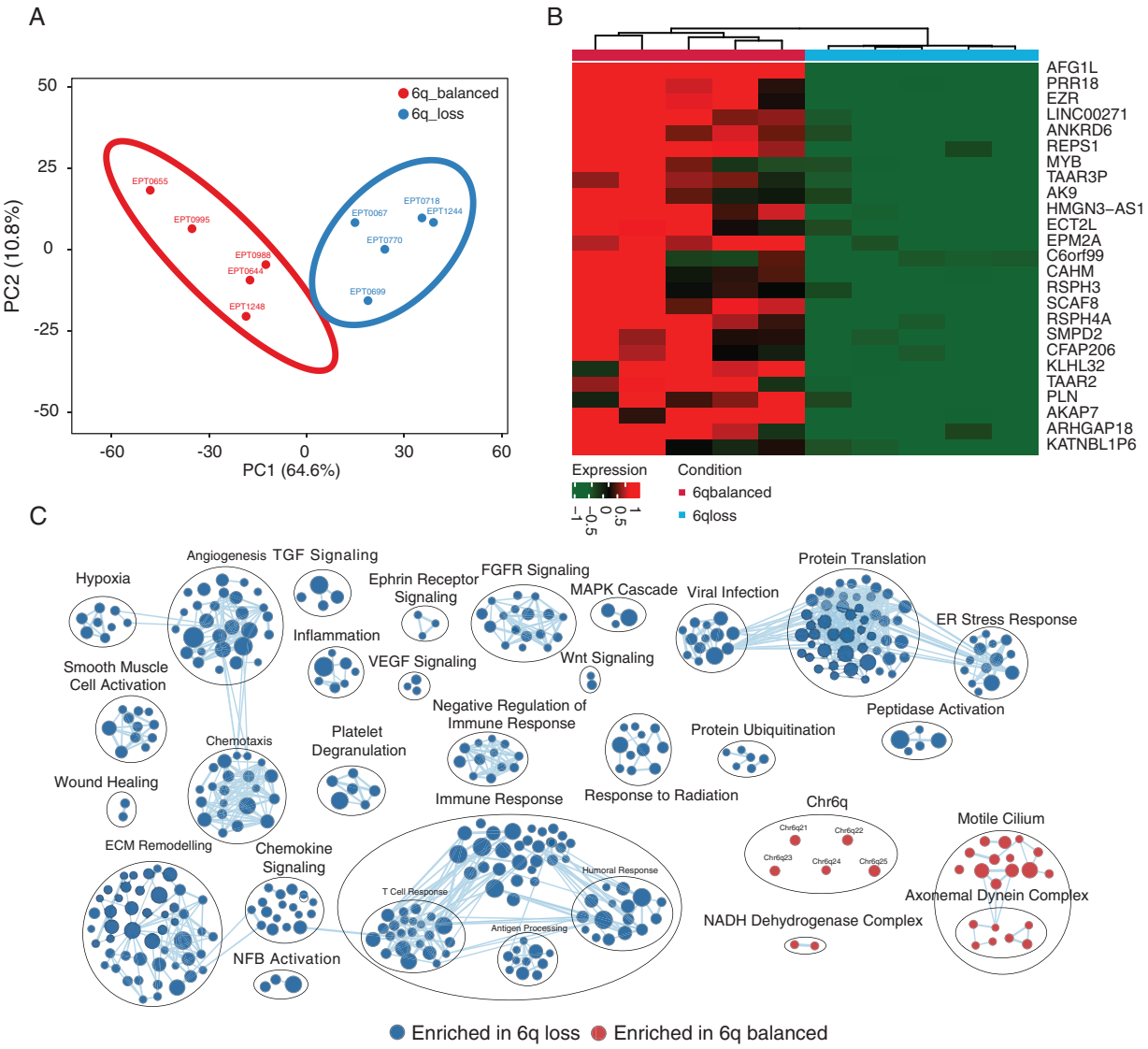

Fig. 3 6q loss as a distinct group. (A) PCA plot of differentially expressed genes ($P_{adj} < .05$) where 6q loss and 6q balanced form separate clusters. Red represents 6q balanced while blue indicates 6q loss. (B) Unsupervised clustering of genes restricted to chromosome 6q. The expression count of the top 25 downregulated genes on chromosome 6q was normalized, scaled, and clustered using Euclidean distance and average linkage metrics. Red denotes upregulation, whereas green represents downregulation. (C) Gene set enrichment results comparing the top significantly enriched pathways and biological processes ($P_{adj} < .01$) between 6q loss and 6q balanced where red indicates enriched in 6q balanced and blue shows enriched in 6q loss.

loss PF-EPN-A as having a similar cell of origin. Our results also support 6q loss PF-EPN-A representing a distinct biological entity, with several distinct pathways, including an increase in hypoxia-related pathways, consistent with recent studies suggesting epigenetic and metabolic reprogramming driving the poor outcome overall of PF-EPN-A tumors.[32] The increased representation of hypoxia-related pathways in 6q loss tumors may potentially account for the poor prognosis, and resistance to radiation therapy, which warrants further investigation.[40] Global levels of H3K27me3 are drastically reduced in PF-EPN-A, and it would be essential to ascertain specific patterns of H3K27me3 immunostaining in 6q loss tumors in future studies.[41,42]

Previously across many non-subgrouped studies, it has been suggested that 6q loss is a marker of excellent survival in ependymoma, highly contrary to our findings.[16,17] This apparent discrepancy is resolved in a group-specific analysis, where 6q loss represents over two-thirds of PF-EPN-B tumors and is non-prognostic; whereas PF-EPN-A has a strong negative prognostic significance. This coupled with our previous findings that 1q gain is not prognostic in PF-EPN-B further emphasize the importance of group-specific analyses when identifying new biomarkers of ependymoma. This is

most evident in the childhood age group where one-third of PF-EPN-A patients fall into high-risk groups (1q gain and/or 6q loss), and most pronounced in the adolescent age group where almost two-thirds of all PF-EPN-A patients fall into a high-risk group, clearly highlighting the critical importance of routine subgrouping.

Recently, the results of ACNS0121 revealed, for the first time in a prospective cohort, that 1q gain PF-EPN-A have a poor prognosis with a 5-year PFS of 35.7% with complete resection and adjuvant radiotherapy, with a propensity to distant rather than local relapses.[11] Although this represents a very poor survival compared to the 81% survival in a completely resected and radiated 1q balanced PF-EPN-A, concerns have arisen regarding the intensification of treatment. Our findings are in keeping with ACNS0121 which suggests that within PF-EPN-A tumors with 1q gain, the outcome is very poor despite aggressive surgery and upfront radiotherapy. Overall, our results are in keeping with those of ACNS0121 where 1q gain tumors recur more frequently in the metastatic compartment, irrespective of 6q loss, suggesting this cytogenetic aberration is a potential driver of metastatic relapse. Considering the poor outcome of this group, the introduction of new upfront approaches can be considered, however, this has been limited by a paucity of promising new agents for PF-EPN-A. Our findings suggest that within PF-EPN-A, 6q loss may represent a significant minority of ubiquitously relapsing patients who may be immediately suitable for a new upfront approach. Conversely, those patients with 1q and 6q balanced PF-EPN-A with complete resection and upfront radiotherapy should not be considered a poor prognostic group as previously suggested, and represent a relatively favorable prognostic group within PF-EPN-A.

Although validation across recently closed prospective trials will be required for confirmation of our findings, the strikingly poor survival of 6q loss group irrespective of treatment and 1q status warrants further evaluation. Analogous to a recent risk stratification of childhood medulloblastoma, this may permit a PF-EPN-A specific risk stratification of intermediate/standard risk, high-risk, and ultra high-risk.[43] Although this would represent relatively low patient numbers, 6q loss PF-EPN-A would represent a group larger than either TP53-mutant SHH (sonic hedgehog) medulloblastoma or MYC-amplified Group 3 medulloblastoma, two groups prioritized for the introduction of novel upfront therapies. In addition to routine subgrouping of PF-EPN-A, the routine use of two cytogenetic markers can form the basis of a simple risk stratification for trials of PF-EPN-A moving forward; whereby 6q loss represents an ultra high-risk group irrespective of treatment and the extent of resection, 1q gain, and incompletely resected tumors represent a high-risk group, with completely resected 1q and 6q balanced tumors representing an intermediate/good prognosis group when receiving postoperative radiotherapy.

Supplementary Material

Supplementary material is available at *Neuro-Oncology* online.

Keywords

1q gain | 6q loss | ependymoma | PFA | PFB | posterior fossa | subgrouping

Funding

L.B. was supported by a Terry Fox International Fellowship and the Meagan's Walk Fellowship in Pediatric Neuro-Oncology. C.L.W. and M.B. are supported by funding from Cancer Australia, the Robert Connor Dawes Foundation, and Carrie's Beanies for Brain Cancer with infrastructure support through the Victorian Government's Operational Infrastructure Support Program. M.D.T. is supported by operating funds from the National Institutes for Health (5R01CA159859-08 and R01NS106155-01) and the Pediatric Brain Tumor Foundation. H.C. is supported by a Garron Family Cancer Centre Fellowship. V.R. and M.D.T. are supported by a Stand Up To Cancer (SU2C) St. Baldrick's Pediatric Dream Team translational research grant (SU2C-AACR-DT1113). V.R. is supported by operating funds from the Canadian Institutes for Health Research, the Brain Tumour Foundation of Canada, the C.R. Younger Foundation, the Garron Family Cancer Centre, Meagan's Walk, b.r.a.i.n.child, and Nelina's Hope. This study was partially funded with support provided by the Government of Ontario, Ministry of Research, Innovation and Science, and the Princess Margaret Cancer Foundation and support from the Princess Margaret Cancer Centre-OICR Translational Genomics Laboratory.

Conflict of interest statement. The authors declare no conflicts of interest.

Authorship statement. Authorship: Experimental design—L.B., L.S., and V.R.; Data collection—L.B., A.H., K.W.P., T.L., T.E.M., R.M., C.F., M.B., C.L.W., S.M.P., M.R.G., T.S.A., E.B., S.K., M.D.T., A.K., K.D.A., D.W.E., M.K., J.R.H., N.G.G., and M.B.; Data analysis—L.B., H.C., A.H., L.S., and V.R.; Interpretation of the data—L.B., L.S., M.D.T., J.R.H., and V.R.; Funding: M.D.T. and V.R.; Manuscript writing—L.B., L.S., E.B., J.R.H., and V.R.

References

1. Khatua S, Ramaswamy V, Bouffet E. Current therapy and the evolving molecular landscape of paediatric ependymoma. *Eur J Cancer*. 2017;70:34–41.
2. Mack SC, Taylor MD. Put away your microscopes: the ependymoma molecular era has begun. *Curr Opin Oncol*. 2017;29(6):443–447.
3. Pajtler KW, Mack SC, Ramaswamy V, et al. The current consensus on the clinical management of intracranial ependymoma and its distinct molecular variants. *Acta Neuropathol*. 2017;133(1):5–12.
4. Cavalli FMG, Hübner JM, Sharma T, et al. Heterogeneity within the PF-EPN-B ependymoma subgroup. *Acta Neuropathol*. 2018;136(2):227–237.

5. Witt H, Mack SC, Ryzhova M, et al. Delineation of two clinically and molecularly distinct subgroups of posterior fossa ependymoma. *Cancer Cell.* 2011;20(2):143–157.
6. Mack SC, Witt H, Piro RM, et al. Epigenomic alterations define lethal CIMP-positive ependymomas of infancy. *Nature.* 2014;506(7489):445–450.
7. Wani K, Armstrong TS, Vera-Bolanos E, et al.; Collaborative Ependymoma Research Network. A prognostic gene expression signature in infratentorial ependymoma. *Acta Neuropathol.* 2012;123(5):727–738.
8. Pajtler KW, Witt H, Sill M, et al. Molecular classification of ependymal tumors across all CNS compartments, histopathological grades, and age groups. *Cancer Cell.* 2015;27(5):728–743.
9. Pajtler KW, Wen J, Sill M, et al. Molecular heterogeneity and CXorf67 alterations in posterior fossa group A (PFA) ependymomas. *Acta Neuropathol.* 2018;136(2):211–226.
10. Ramaswamy V, Hielscher T, Mack SC, et al. Therapeutic impact of cytoreductive surgery and irradiation of posterior fossa ependymoma in the molecular era: a retrospective multicohort analysis. *J Clin Oncol.* 2016;34(21):2468–2477.
11. Merchant TE, Bendel AE, Sabin ND, et al. Conformal radiation therapy for pediatric ependymoma, chemotherapy for incompletely resected ependymoma, and observation for completely resected, supratentorial ependymoma. *J Clin Oncol.* 2019;37(12):974–983.
12. Zapotocky M, Beera K, Adamski J, et al. Survival and functional outcomes of molecularly defined childhood posterior fossa ependymoma: cure at a cost. *Cancer.* 2019;125(11):1867–1876.
13. Andreiuolo F, Le Teuff G, Bayar MA, et al.; SIOP Ependymoma Biology Working Group BIOMECA (BIOlogical Markers for Ependymomas in Children and Adolescents). Integrating Tenascin-C protein expression and 1q25 copy number status in pediatric intracranial ependymoma prognostication: a new model for risk stratification. *PLoS One.* 2017;12(6):e0178351.
14. Kilday JP, Mitra B, Domerg C, et al. Copy number gain of 1q25 predicts poor progression-free survival for pediatric intracranial ependymomas and enables patient risk stratification: a prospective European clinical trial cohort analysis on behalf of the Children's Cancer Leukaemia Group (CCLG), Societe Francaise d'Oncologie Pediatrique (SFOP), and International Society for Pediatric Oncology (SIOP). *Clin Cancer Res.* 2012;18(7):2001–2011.
15. Upadhyaya SA, Robinson GW, Onar-Thomas A, et al. Molecular grouping and outcomes of young children with newly diagnosed ependymoma treated on the multi-institutional SJYC07 trial. *Neuro Oncol.* 2019;21(10):1319–1330.
16. Korshunov A, Witt H, Hielscher T, et al. Molecular staging of intracranial ependymoma in children and adults. *J Clin Oncol.* 2010;28(19):3182–3190.
17. Puget S, Grill J, Valent A, et al. Candidate genes on chromosome 9q33-34 involved in the progression of childhood ependymomas. *J Clin Oncol.* 2009;27(11):1884–1892.
18. Carter M, Nicholson J, Ross F, et al. Genetic abnormalities detected in ependymomas by comparative genomic hybridisation. *Br J Cancer.* 2002;86(6):929–939.
19. Grill J, Avet-Loiseau H, Lellouch-Tubiana A, et al. Comparative genomic hybridization detects specific cytogenetic abnormalities in pediatric ependymomas and choroid plexus papillomas. *Cancer Genet Cytogenet.* 2002;136(2):121–125.
20. Ward S, Harding B, Wilkins P, et al. Gain of 1q and loss of 22 are the most common changes detected by comparative genomic hybridisation in paediatric ependymoma. *Genes Chromosomes Cancer.* 2001;32(1):59–66.
21. Scheil S, Brüderlein S, Eicker M, et al. Low frequency of chromosomal imbalances in anaplastic ependymomas as detected by comparative genomic hybridization. *Brain Pathol.* 2001;11(2):133–143.
22. Hirose Y, Aldape K, Bollen A, et al. Chromosomal abnormalities subdivide ependymal tumors into clinically relevant groups. *Am J Pathol.* 2001;158(3):1137–1143.
23. Reardon DA, Entrekin RE, Sublett J, et al. Chromosome arm 6q loss is the most common recurrent autosomal alteration detected in primary pediatric ependymoma. *Genes Chromosomes Cancer.* 1999;24(3):230–237.
24. Monoranu CM, Huang B, Zangen IL, et al. Correlation between 6q25.3 deletion status and survival in pediatric intracranial ependymomas. *Cancer Genet Cytogenet.* 2008;182(1):18–26.
25. Capper D, Jones DTW, Sill M, et al. DNA methylation-based classification of central nervous system tumours. *Nature.* 2018;555(7697):469–474.
26. Hovestadt V, Remke M, Kool M, et al. Robust molecular subgrouping and copy-number profiling of medulloblastoma from small amounts of archival tumour material using high-density DNA methylation arrays. *Acta Neuropathol.* 2013;125(6):913–916.
27. Sturm D, Witt H, Hovestadt V, et al. Hotspot mutations in H3F3A and IDH1 define distinct epigenetic and biological subgroups of glioblastoma. *Cancer Cell.* 2012;22(4):425–437.
28. Cavalli FMG, Remke M, Rampasek L, et al. Intertumoral heterogeneity within medulloblastoma subgroups. *Cancer Cell.* 2017; 31(6):737–754.e736.
29. Kim D, Paggi JM, Park C, Bennett C, Salzberg SL. Graph-based genome alignment and genotyping with HISAT2 and HISAT-genotype. *Nat Biotechnol.* 2019;37(8):907–915.
30. Liao Y, Smyth GK, Shi W. featureCounts: an efficient general purpose program for assigning sequence reads to genomic features. *Bioinformatics.* 2014;30(7):923–930.
31. Reimand J, Isserlin R, Voisin V, et al. Pathway enrichment analysis and visualization of omics data using g:Profiler, GSEA, Cytoscape and EnrichmentMap. *Nat Protoc.* 2019;14(2):482–517.
32. Michealraj KA, Kumar SA, Kim LJY, et al. Metabolic regulation of the epigenome drives lethal infantile ependymoma. *Cell.* 2020;181(6):1329–1345.e24.
33. Winter SC, Buffa FM, Silva P, et al. Relation of a hypoxia metagene derived from head and neck cancer to prognosis of multiple cancers. *Cancer Res.* 2007;67(7):3441–3449.
34. Mense SM, Sengupta A, Zhou M, et al. Gene expression profiling reveals the profound upregulation of hypoxia-responsive genes in primary human astrocytes. *Physiol Genomics.* 2006;25(3):435–449.
35. Harris AL. Hypoxia–a key regulatory factor in tumour growth. *Nat Rev Cancer.* 2002;2(1):38–47.
36. Gross C, Dubois-Pot H, Wasylyk B. The ternary complex factor Net/Elk-3 participates in the transcriptional response to hypoxia and regulates HIF-1 alpha. *Oncogene.* 2008;27(9):1333–1341.
37. Elvidge GP, Glenny L, Appelhoff RJ, Ratcliffe PJ, Ragoussis J, Gleadle JM. Concordant regulation of gene expression by hypoxia and 2-oxoglutarate-dependent dioxygenase inhibition: the role of HIF-1α, HIF-2α, and other pathways. *J Biol Chem.* 2006;281(22):15215–15226.
38. Buffa FM, Harris AL, West CM, Miller CJ. Large meta-analysis of multiple cancers reveals a common, compact and highly prognostic hypoxia metagene. *Br J Cancer.* 2010;102(2):428–435.
39. Lalonde E, Ishkanian AS, Sykes J, et al. Tumour genomic and microenvironmental heterogeneity for integrated prediction of 5-year biochemical recurrence of prostate cancer: a retrospective cohort study. *Lancet Oncol.* 2014;15(13):1521–1532.
40. Rockwell S, Dobrucki IT, Kim EY, Marrison ST, Vu VT. Hypoxia and radiation therapy: past history, ongoing research, and future promise. *Curr Mol Med.* 2009;9(4):442–458.
41. Panwalkar P, Clark J, Ramaswamy V, et al. Immunohistochemical analysis of H3K27me3 demonstrates global reduction in group-A childhood posterior fossa ependymoma and is a powerful predictor of outcome. *Acta Neuropathol.* 2017;134(5):705–714.
42. Bayliss J, Mukherjee P, Lu C, et al. Lowered H3K27me3 and DNA hypomethylation define poorly prognostic pediatric posterior fossa ependymomas. *Sci Transl Med.* 2016; 8(366):366ra161.
43. Ramaswamy V, Remke M, Bouffet E, et al. Risk stratification of childhood medulloblastoma in the molecular era: the current consensus. *Acta Neuropathol.* 2016;131(6):821–831.